Meteorologische Zeitschrift, Vol. **24**, No. 5, 465–480 (published online July 16, 2015)

Influence of large offshore wind farms on North German climate

Marita Boettcher[1*], Peter Hoffmann[2,3], Hermann-J. Lenhart[4], K. Heinke Schlünzen[1] and Robert Schoetter[2,5]

[1]Meteorological Institute, CEN, University of Hamburg, Germany
[2]formerly: Meteorological Institute, CEN, University of Hamburg, Germany
[3]now: Department of Mathematics, University of Hamburg, Germany
[4]Department of Informatics, Research Group Scientific Computing, University of Hamburg, Germany
[5]now: CNRM-GAME, Meteo France, Toulouse, France

(Manuscript received September 30, 2014; in revised form February 27, 2015; accepted April 24, 2015)

Abstract

Wind farms impact the local meteorology by taking up kinetic energy from the wind field and by creating a large wake. The wake influences mean flow, turbulent fluxes and vertical mixing. In the present study, the influences of large offshore wind farms on the local summer climate are investigated by employing the mesoscale numerical model METRAS with and without wind farm scenarios. For this purpose, a parametrisation for wind turbines is implemented in METRAS. Simulations are done for a domain covering the northern part of Germany with focus on the urban summer climate of Hamburg. A statistical-dynamical downscaling is applied using a skill score to determine the required number of days to simulate the climate and the influence of large wind farms situated in the German Bight, about 100 km away from Hamburg.

Depending on the weather situation, the impact of large offshore wind farms varies from nearly no influence up to cloud cover changes over land. The decrease in the wind speed is most pronounced in the local areas in and around the wind farms. Inside the wind farms, the sensible heat flux is reduced. This results in cooling of the climate summer mean for a large area in the northern part of Germany. Due to smaller momentum fluxes the latent heat flux is also reduced. Therefore, the specific humidity is lower but because of the cooling, the relative humidity has no clear signal. The changes in temperature and relative humidity are more wide spread than the decrease of wind speed. Hamburg is located in the margins of the influenced region. Even if the influences are small, the urban effects of Hamburg become more relevant than in the present and the off-shore wind farms slightly intensify the summer urban heat island.

Keywords: local climate, urban climate, regional climate, wind energy, urban heat island, numerical model

1 Introduction

Wind turbines become more and more important to generate electricity since their CO_2 footprint is small. They extract kinetic energy from the flow and convert it into electric energy. The wind speed is thereby reduced in the wake of a wind turbine and turbulence is increased. The single wakes of several wind turbines in a wind farm interact and cause a large single wake for one wind farm through superposition. The length of the wake depends on the atmospheric stability and therefore the temperature profile, the ambient turbulence and the surface roughness, because these quantities affect the vertical mixing (Emeis, 2010). The smooth surface and reduced atmospheric turbulence around offshore wind farms lead to a wake which is in neutral cases about three times longer than for onshore wind farms (Emeis, 2010). Analyses of wakes resulting from wind farms located in the North Sea and the Baltic Sea show a measurable downwind influence on the wind field up to distances of several tens of kilometres (Christiansen and Hasager, 2005). For onshore wind farms, Fitch et al. (2013) found a 10 % deficit in wind speed 60 km downwind of the wind farms during nighttime.

The reduced wind speed and the associated wind shear in the wake induces atmospheric mixing. As a result, air from aloft is entrained increasing the lower wind speed in the wake. Due to the turbulent exchange, the area of reduced wind speed is vertically extended. This leads to lower wind speeds in levels well above the wind farm (Baidya Roy et al., 2004). Furthermore, the dynamic pressure in front of each rotor leads to an increase of the wind speed below the rotor, close to the surface (Baidya Roy et al., 2004). Through this, the vertical mixing is increased and this also affects the surface fluxes and mixes the vertical temperature profile (Baidya Roy and Traiteur, 2010). Because of these effects on the vertical exchange, a multitude of very large wind farms is able to change the global mean temperature as found from global model simulations whereas a cooling is found for offshore and a warming

*Corresponding author: Marita Boettcher, Meteorological Institute, CEN, University of Hamburg, Bundesstraße 55, 20146 Hamburg, Germany, e-mail: marita.boettcher@uni-hamburg.de

DOI 10.1127/metz/2015/0652

Gebrüder Borntraeger Science Publishers, Stuttgart, www.borntraeger-cramer.com

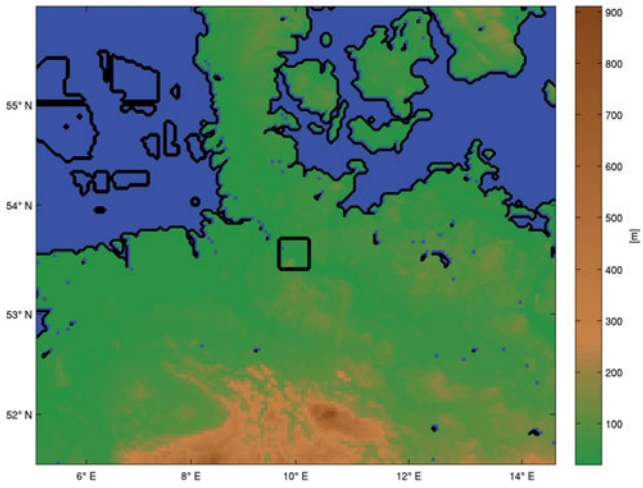

Figure 1: Orography of the model domain. Hamburg is located in the domain centre and marked with a black frame. The wind farms in the German Bight are also outlined with black frames and located in the North-West quadrant of the model domain.

for onshore installations (Wang and Prinn, 2010). Regional changes generated by such very large wind farms can be in the order of up to ±2 K (Keith et al., 2004). In addition, the global distribution of rainfall and clouds may be changed (Wang and Prinn, 2010). In very extreme cases with energy extraction in the range of terawatts, the global atmospheric motion can be affected and may result in global climate effects (Miller et al., 2011).

In the present study, the impact of large offshore wind farms in the German Bight on regional summer climate is investigated using the meteorological model METRAS. The changes in the climate caused by the proposed wind farms are determined for North-Western Germany and with respect to Hamburg. Hamburg is located in the centre of the model domain (Figure 1).

Hamburg has a maritime climate with moderately warm and moist weather conditions. With climate change, a warmer climate can be expected (Daschkeit, 2011). Therefore, adaptation measures for reduction of heat stress and the urban heat island become more important also for Hamburg. Schlünzen et al. (2010) showed that the urban heat island of Hamburg is most relevant during the summer months, and it will probably not change in future climate (Hoffmann and Schlünzen, 2013) if the urban morphology is not changed. The present study investigates if one of the possible CO_2 mitigation measures, namely energy production by offshore wind farms in the German Bight, impacts the summer climate of Hamburg. As a consequence of the changed flow field over the German Bight, changes in the development of mesoscale meteorological systems such as the land sea breeze or the track of a cyclone may be possible. This may cause changes not only in the wake of the wind farms up to a distance of several tens of kilometres downwind, but also in a much larger area up to several hundreds of kilometres. In the focus of the current study is if the urban climate of Hamburg, a city situated about 100 kilometres inland from the coast, could be influenced by the wind farms in the German Bight.

To represent the climatological mean, simulations of typical weather situations are performed and the results are averaged. The methods, data and model used in the present study are described in Section 2. The results are discussed in Section 3. Conclusions are drawn in Section 4.

2 Methods and data

In the present study, different weather situations are simulated using the numerical mesoscale model METRAS (Section 2.1). The model is extended to account for wind farm effects (Section 2.2). The model domain and wind farm data are described in Section 2.3. The weather situations are the same as introduced in the weather pattern classification of Hoffmann and Schlünzen (2013). A statistical skill score is used in the present study to determine if the climatological frequency distributions of the selected meteorological variables are represented (Section 2.4) and thus the selected cases do indeed represent climatological data of the summer. Section 2.5 shows that the simulated sensible and latent heat fluxes resemble the measurements of the fluxes in the German Bight.

2.1 Mesoscale atmospheric model METRAS

METRAS (Schlünzen, 1990; Schlünzen et al., 2012) is a non-hydrostatic, three-dimensional, numerical model of the atmosphere, used in the present study to determine the influence of large offshore wind farms on meteorology. The relevant model characteristics are shortly summarised below.

The basic equations for momentum, temperature and humidity are solved in flux form on a terrain following Arakawa-C grid. The equations are Reynolds averaged, and the anelastic and the Boussinesq approximations are used (Schlünzen, 1990). The turbulent fluxes resulting from Reynolds averaging are parametrised with a first order closure. The turbulent exchange coefficients are calculated with a mixing length approach for stable stratification and consider a counter gradient term for unstable stratification (Lüpkes and Schlünzen, 1996). The momentum advection is solved using the Adams-Bashfort scheme with second order central differences in space. A seven point filter is used to smooth the short waves resulting from this numerical scheme. The advection of scalars is solved with a first order upstream scheme. Depending on the time step needed for the different processes in the model, the vertical diffusion is solved either explicit or with the semi-implicit Crank-Nicholson scheme. For taking account of sub-grid scale surface cover effects, each grid cell may include up to ten surface cover classes. A flux aggregation method is

used to determine the vertical fluxes close to the surface (von Salzen et al., 1996). Due to the 4 km horizontal grid resolution used in this study, sub-grid scale surface cover effects and the connected surface fluxes are important. Therefore, the flux aggregation method is used in the whole domain, also in the urban areas, instead of the coupled urban parametrisation scheme BEP (Grawe et al., 2013). The different surface cover classes differ in albedo, thermal diffusivity, thermal conductivity, water availability, water saturation values and roughness lengths; typical initial values are given in Schlünzen and Katzfey (2003).

For the present simulations, METRAS is forced with ECMWF analysis data (ECMWF, 2009; ECMWF, 2010) using the nudging approach. Simulations with initialisation date after 26 January 2010 are nudged with 16 km resolution data, before with 25 km resolution data. Nudging is done at the lateral boundaries. The variables that are nudged are the horizontal wind components, the temperature and the humidity. A nudging term is added to these equations. The nudging term is larger at the lateral boundaries and decreases towards the inner model domain. It becomes nearly zero five grid cells away from the lateral boundaries.

Cloud water and rain water are not forced, but the ECMWF data of these are added to the specific humidity values at the lateral boundaries to allow for smaller scale cloud developments in the nudged model METRAS. At the surface, the budget equations for temperature and humidity are solved. For the wind components a no slip condition is applied. The falling of rain water is explicitly calculated (including evaporation). Rain at the first grid level is assumed to reach the ground. Clouds close to the ground are also assumed to reach the ground. At the model top, the horizontal wind components are nudged while the vertical wind component is set to zero. For the other variables mentioned before, zero gradient boundary conditions are applied.

The water temperatures are prescribed from the NOAA Optimum Interpolation Sea Surface Temperature V2 (Reynolds et al., 2002) and interpolated to the METRAS grid. The water temperatures are corrected for the local altitude to determine the water temperature for inland water bodies. For the soil temperatures, the same values are taken. Initial surface temperatures are taken and interpolated from ECMWF analysis data (ECMWF, 2009; ECMWF, 2010).

The three-dimensional version of METRAS employs a balanced basic state profile that is consistent with the averaged profile of the ECMWF analysis data. This basic state is also the initial profile and extended to the whole model domain assuming horizontal homogeneity. The diastrophy method with orography growing is used (Pielke, 1984). Within the first 1.5 hours of integration intense nudging imposes the heterogeneous large scale situation. The initialisation phase takes about 3 hours to ensure a heterogeneous meteorology consistent with the forcing data.

The model simulations start for 2000 local time (LT) of the initialisation day. The first update of the forcing data takes place 4 hours later. After that, the forcing data are updated every six hours. Between two updating times, forcing data are linearly interpolated (Schlünzen et al., 2011). The model is integrated for a period of three days and four hours for each simulation.

METRAS has successfully been applied to the German Bight and the northern part of Germany before (Schlünzen, 1990; Schlünzen, 1997; Schlünzen et al., 1997; von Salzen and Schlünzen, 1999; Meyer and Schlünzen, 2011). The model applied here has been extended with the actuator disc concept to represent the effects of wind turbines.

2.2 Parametrisation of wind turbines

Wind turbines are not resolved in models but its effects are parametrised. Several approaches to consider the impact of wind turbines in atmospheric models are discussed in the literature. High resolution models designed for wind turbine load and interactions between wind turbines use an explicit consideration of the forces acting on the rotor (Fitch et al., 2012; Gross, 2010) while regional and global models with a coarse resolution parametrise wind farms through enlarged roughness length (Keith et al., 2004; Fitch et al., 2012; Wang and Prinn, 2010). An intermediate parametrisation between these two approaches is to consider wind turbines or wind farms by a sink of kinetic energy, done by an additional term to the momentum equations (El Kasmi and Masson, 2008; Fitch et al., 2012; Fitch et al., 2013; Linde, 2011). In this parametrisation, the effects of wind turbines and wind farms are modelled at hub hight, which permit a flow around the wind turbines and wind farms. Hence, the parametrisation is more realistic as the roughness length approach but less computational expensive than explicit consideration of the forces. The intermediate parametrisation is used for this study. The parametrisation is realised with the actuator disc concept (ADC). In the ADC, a wind turbine rotor is described as an infinitesimal thin disc with the size and position of the rotor. Betz published in 1926 the concept based on the conservation law for momentum and mass for a laminar and frictionless flow (Hau, 2002; Molly, 1978). This concept is used here.

Figure 2 shows a schematic diagram of the ADC. The kinetic energy of the air depends on the velocity. Far upwind of a wind turbine, the air flux is not influenced by the wind turbine and has the mean speed v_1. Due to the extraction of kinetic energy, the mean flow speed v_2 downwind of a wind turbine is reduced. The wind speeds v_1 and v_2 are averaged for the rotor parallel areas A_1 and A_2 up- and downwind of the rotor (area A'). The pressure in front of the rotor increases because of the wind speed reduction. The parallel streamlines of the laminar flow spread. The air which passed the small area A_1 far upwind of the wind turbine passes a larger area A_2

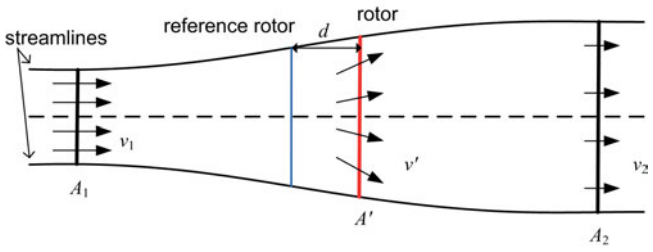

Figure 2: Schematic diagram of the actuator disc concept. The mean wind speed upwind, at and downwind of a wind turbine rotor is denoted with v_1, v' and v_2. The corresponding areas are given with A_1, A' and A_2. The distance between the rotor and the reference rotor is given with d.

far downwind of the wind turbine. The maximal thrust $T_{\max}$ is reached for $v_2 = 0$. Within this conceptual model the dimensionless thrust coefficient c_T only depends on mean wind speed and can be formulated which is the percentage of rotor thrust T' to maximum thrust $T_{\max}$ for an air density ρ (Eq. (2.1)).

$$c_T = \frac{T'}{T_{\max}} = \frac{\frac{1}{2}\rho A' \left(v_1^2 - v_2^2\right)}{\frac{1}{2}\rho A' v_1^2} = 1 - \frac{v_2^2}{v_1^2} \qquad (2.1)$$

The thrust coefficient c_T is a parameter for a given wind turbine type. It is provided by the wind turbine manufacturers or can be determined from field measurements by applying Eq. (2.1). The thrust coefficient varies with mean wind speed. According to the definition of the thrust coefficient by Mikkelsen (2003), the rotor thrust in Eq. (2.2) only depends on the mean wind speed of the undisturbed flow, the thrust coefficient and the rotor area. Since the rotor area can be easily calculated by using the given rotor diameter D, only the mean undisturbed wind speed has to be determined to apply Eq. (2.2). This equation is used in the numerical model.

$$T' = \frac{1}{2}\rho A' \left(v_1^2 - v_2^2\right) = c_T T_{\max} = \frac{1}{2} c_T \rho A' v_1^2 \qquad (2.2)$$

The undisturbed wind speed is calculated using a so named reference rotor in some distance upwind of the actual rotor. Prospathopoulos (2010) and Linde (2011) showed that the best results are achieved when choosing a distance d of 1.0 or 0.1 times rotor diameter D upwind of the wind turbine, respectively. In this area, the wind speed and the wind direction are already slightly disturbed. However, choosing a position further upwind decouples the wind speed and direction at rotor and reference rotor position, especially in complex terrain. The choice of the reference rotor position $d = 0.1D$ produces a smaller error than the position $d = 1.0D$ as shown by Linde (2011) using an obstacle resolving microscale model.

In a mesoscale model, horizontal grid sizes are typically large compared to the size of a wind turbine rotor. Therefore, the rotor and the reference rotor are in general in the same grid cell for a single wind turbine. Furthermore, several wind turbines might be located within one grid cell in the horizontal and then wakes are superposed to one large wake. The vertical grid size is typically less coarse. Therefore, a rotor is represented at its real hub height, usually within several vertical grid cells. A whole wind farm is located in just a few adjacent grid cells. Therefore, to determine the average reference wind speed in METRAS for each wind farm, the wind speed of all grid cells containing the same wind farm are averaged. This averaged value is then used to be the undisturbed upwind wind speed.

The part of the grid cell that is covered by a rotor is defined by a wind turbine mask. Multiplying Eq. (2.2) with the wind turbine mask and subtracting this term from the basic equation of momentum leads to the parametrisation for wind turbines. Since the thrust coefficient c_T depends on mean wind speed v_1, the wind turbines switch on and off autonomously, if the wind speed becomes higher or lower than the cut-in or cut-off velocity.

Compared to the coarse grid of a mesoscale model, the tower of a wind turbine is small. More than three rotor diameters downwind, the shape of the wake is mainly determined by the influence of the rotor. The influence of the tower on the wake is negligible in this area (Linde, 2011). Therefore, the towers of the wind turbines are neglected in the present study. With these assumptions and by using the ADC, several large wind farms can be represented in the model domain.

Due to a lack of ground based measurements in the wake of large offshore wind farms, the model is verified against other models and satellite data. Simulations with this parametrisation give plausible results of the offshore wind farm Horns Rev (not shown) against the satellite data in Christiansen and Hasager (2005). The model also achieved plausible results redoing the idealised simulations of the model COSMO of an offshore wind farm from Stütz et al. (2012) and the single onshore wind turbine Nibe B with the model MITRAS of Linde (2011).

2.3 Model domain

The model covers a domain from about 50 ° 47 ′ N to 56 ° 25 ′ N and from about 4 ° 26′ E to 15 ° 40′ E, which corresponds to an area of 700 × 628 km^2 (Figure 1). This includes Northern Germany and the German Bight as well as parts of The Netherlands, Denmark, Sweden, Poland and the Baltic Sea. Hamburg is located in the centre of the model domain (marked with a black frame in Figure 1). The wind farms planned in the German Bight are projected to be found in the North-West part of the domain and cover a considerable part of the area. The horizontal grid size is 4 km. The vertical grid resolution in the lowest 100 m is 20 m, with the lowest grid level at 10 m above ground. Above, the vertical grid size increases with an increasing factor of 1.175 per grid cell. The maximum grid size is 1000 m above 5000 m. The domain includes 34 model levels with 19 levels located

within the lowest 2000 m. The model top is at 12000 m. Due to the high vertical grid resolution, the momentum absorption of the wind turbines is considered in their corresponding hub height.

Data describing the position of the proposed wind farms are taken from the "Zukunft Küste – Coastal Futures" project (Burkhard, 2006; Lange et al., 2010). Following the extreme scenario "B1 – the North Sea is primarily used as energy park" 90 GW installed power are proposed to be installed in the German Bight until the year 2055. The average power of a single wind turbine is assumed to be 10 MW. This leads to a total number of 9000 wind turbines located in 25 wind farms. For the simulations discussed in the present work, the wind turbines are placed in a distance of 1990 m from each other in each direction without considering the main wind direction. This leads to exactly 9000 wind turbines in the proposed area (Figure 1). To avoid effects from the model boundaries, the wind farms are placed at least four grid cells away from the lateral boundaries.

The technical specification for wind turbines that produce 10 MW is yet not clear. Therefore, the thrust coefficient is deduced from accessible measurements of a Nordex N80/2500 wind turbine for a standard density of the air (Machielse et al., 2007). The determination of the thrust coefficient is given in the Appendix. A hub height of 80 m is assumed.

2.4 Simulated weather situations

For quantification of the impact of large wind farms in the German Bight on the summer climate, the climate mean needs to be simulated. The computational costs to simulate 30 years on a $4 \times 4\,\mathrm{km}^2$ grid would be too large, therefore only a selection of typical weather situations occurring in the summer season are simulated. The statistic-dynamical downscaling method for simulating the urban heat island (UHI) of Hamburg of Hoffmann and Schlünzen (2013) is used as a base. The simulations from this study are extended to represent the climate summer mean of Northern Germany by a number of additional simulations. The number of necessary additional simulations is determined by a skill score (SSP) following Perkins et al. (2007). The SSP is also used to evaluate the simulated frequency distributions of hourly values.

Hoffmann and Schlünzen (2013) developed the statistical-dynamical downscaling method for simulating the UHI of Hamburg with METRAS. There are several comparison studies showing that there is no best weather pattern classification (WPC) and that WPC should be "viewed as purpose-made" (Huth et al., 2008). Therefore, each target parameter requires the construction of its own optimal classification. The WPC used here is especially developed for representing the mean strong UHI of Hamburg. A detailed discussion about the choice of the classification is given in Hoffmann and Schlünzen (2013).

Seven weather patterns (WP), important for the UHI, were found through the WPC by clustering 700 hPa fields from the ERA40-reanalysis using the k-means based clustering method SANDRA (simulated annealing and diversified randomization, Philipp et al. (2007)). Due to the low number of WP, the explained UHI variance was not high enough if only days close to the cluster centre were simulated (Hoffmann, 2012). Therefore, Hoffmann (2012) subdivided the WP according to the strength of the UHI within each WP. Consequential, two weather situations are simulated for each WP. These represent the maximum and the threshold UHI. The threshold UHI is 3 K and refers to the magnitude of the UHI. For planning adaptation measures only strong UHI days are interesting because these are situations where temperatures can be reduced using such measures. Hence, this method simulates the mean strong UHI of Hamburg (UHI > 3 K). The seven weather situations representing the maximum UHI inside each WP are denoted with WP1M to WP7M. The seven threshold weather situations are named WP1T to WP7T. WP7M and WP7T refer to the same weather situation. Consequently, the mean strong UHI of Hamburg is calculated from thirteen different simulations by statistical recombination (Hoffmann, 2012).

To extend the thirteen simulations of Hoffmann (2012) to represent the climatological summer mean for Northern Germany additional to the mean strong UHI of Hamburg, preferably more than thirteen simulations are used. Therefore, the simulations of Hoffmann (2012) are completed by simulations for the meteorological situation closest to the seven cluster centres (WP1C to WP7C) and used as the reference simulations for the current condition without wind farms in the German Bight. For each simulated situation a two day period is evaluated, therefore 40 days are available in total to represent the climatological summer mean. To ensure that these 40 days are sufficient, a test with a statistical skill score following Perkins et al. (2007) is applied. The SSP compares two frequency distributions and is equal one if both distributions are the same and is equal zero if both distributions have no overlap. Perkins et al. (2007) state that for SSP > 0.8 the agreement is "considerable" and for SSP = 0.9 the agreement is "near-perfect". Therefore, the frequency distributions are defined to be represented reasonable well in the present study if the SSP is larger than 0.8. This means that more than 80 % of the frequency distributions overlap.

The data from 27 weather stations in Germany and The Netherlands include hourly observations over 30 years from 1981 to 2010. The investigations have been done for each weather station separately. Analysis is done for the frequency distributions of wind speed and temperature because they are most important to quantify the impact of wind farms on climate. The frequency distributions are built using 1 m/s bins for wind speed and 1 K bins for the temperature. The number of days needed to represent these frequency distributions is the required number of days for representing the summer

climate. The bootstrap resampling method is used in order to create thousand pairs of frequency distributions from which the SSP is calculated.

The mean SSP for 40 randomly chosen days from measurements is in the range of 0.91 to 0.95 for wind speed with a mean of 0.94 (Figure 3a). For temperature, the mean SSP is 0.91 with the range of 0.89 to 0.91 (Figure 3b). Therefore, the SSP for 40 days is clearly higher than 0.8 and thus close to a "near-perfect" agreement as defined by Perkins et al. (2007).

In contrast to the SSP test, the simulated 40 days are not independent from each other, but always two consecutive days are simulated. Furthermore, the situations are chosen by a WPC involving the occurrence of the WP, even if the SSP expects randomly chosen days. For wind speed, the mean SSP is 0.87 which is slightly below the range for wind speed of 40 randomly chosen days. For temperature, the mean SSP is 0.90 and thus similar to the SSP for temperature of 40 randomly chosen days. The SSPs are shown in Figure 3a for wind speed and in Figure 3b for temperature for all 27 weather stations. For wind speed the SSP is lower for the chosen 40 days than for randomly selected 40 days at 13 out of the 27 sites, but only one of these stations (Cuxhaven) is close to the German Bight. Thus, the representation of the summer climate is estimated to be at least sufficient. For temperature, the SSP of the chosen 40 days fits the range of the randomly chosen 40 days except for Gardelegen, again one site not close to the German Bight. The SSPs for wind speed and temperature are both higher than 0.8.

Figure 3c shows the SSP of the model results against the chosen 40 days. The SSP for wind speed is in the range of 0.66 to 0.90 and for temperature from 0.73 to 0.90. The mean SSP is 0.83 for both and therefore a good result (Perkins et al., 2007). Thus, the 40 chosen weather situations and the following model results represent the climate summer mean for Northern Germany. Calculating the mean strong UHI following Hoffmann (2012), the results of these simulations are also usable to investigate in the impact of large offshore wind farm to the UHI of Hamburg.

2.5 Simulated sensible and latent heat fluxes in the German Bight

The air temperature in Northern Germany is impacted by the sea surface temperature of the German Bight. Therefore, the simulated sensible heat flux between water and atmosphere is important for correctly simulating the summer climate. For the German Bight during summer months (June, July and August) the monthly mean sensible heat flux is slightly positive, means warming the atmosphere, in the range of 2 W/m^2 to 12 W/m^2 with higher values at the coast and lower values at the open sea (Becker, 1981; Michaelsen et al., 1998; Schlünzen and Krell, 2004). In Figure 4a, the simulated mean sensible heat flux averaged for the reference simulations is shown. The result fits very well with the data from Michaelsen et al. (1998).

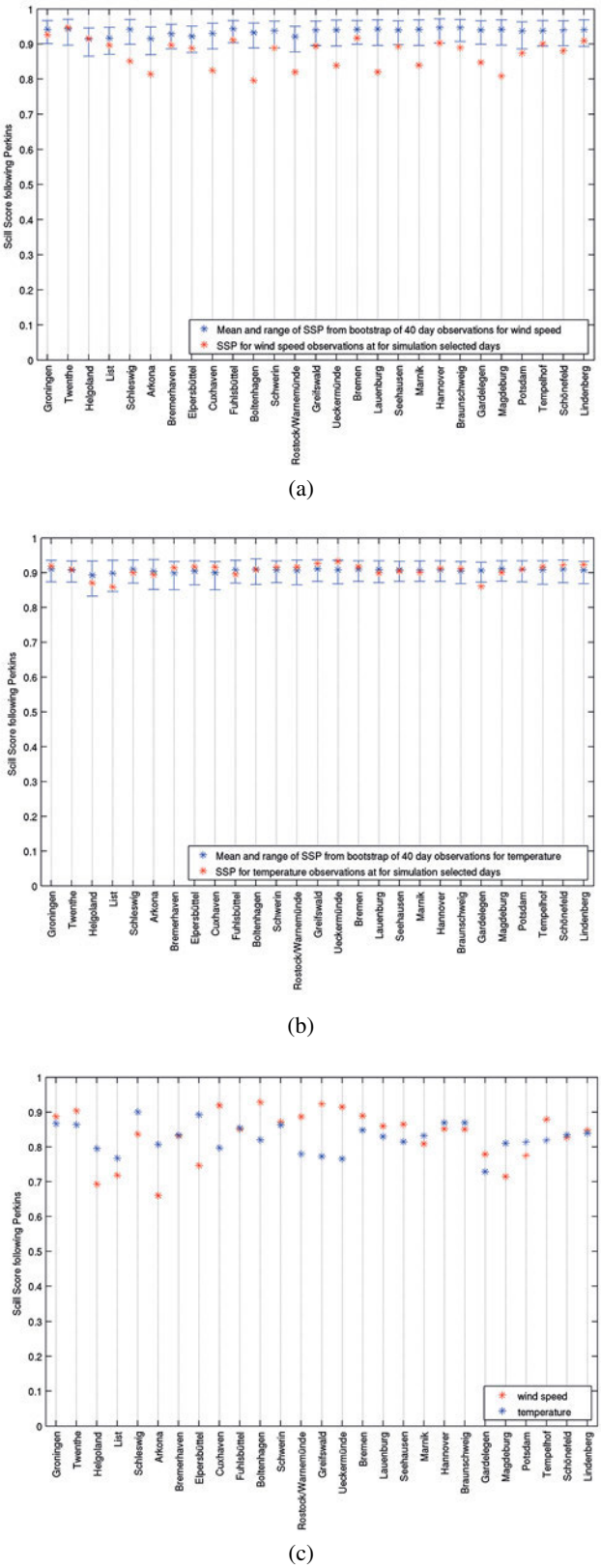

Figure 3: Skill Score following Perkins for individual meteorological sites for (a) wind speed and (b) temperature based on 30 years of hourly data. (c) Skill Score following Perkins for individual meteorological sites for wind speed and temperature based on model results and the chosen 40 days.

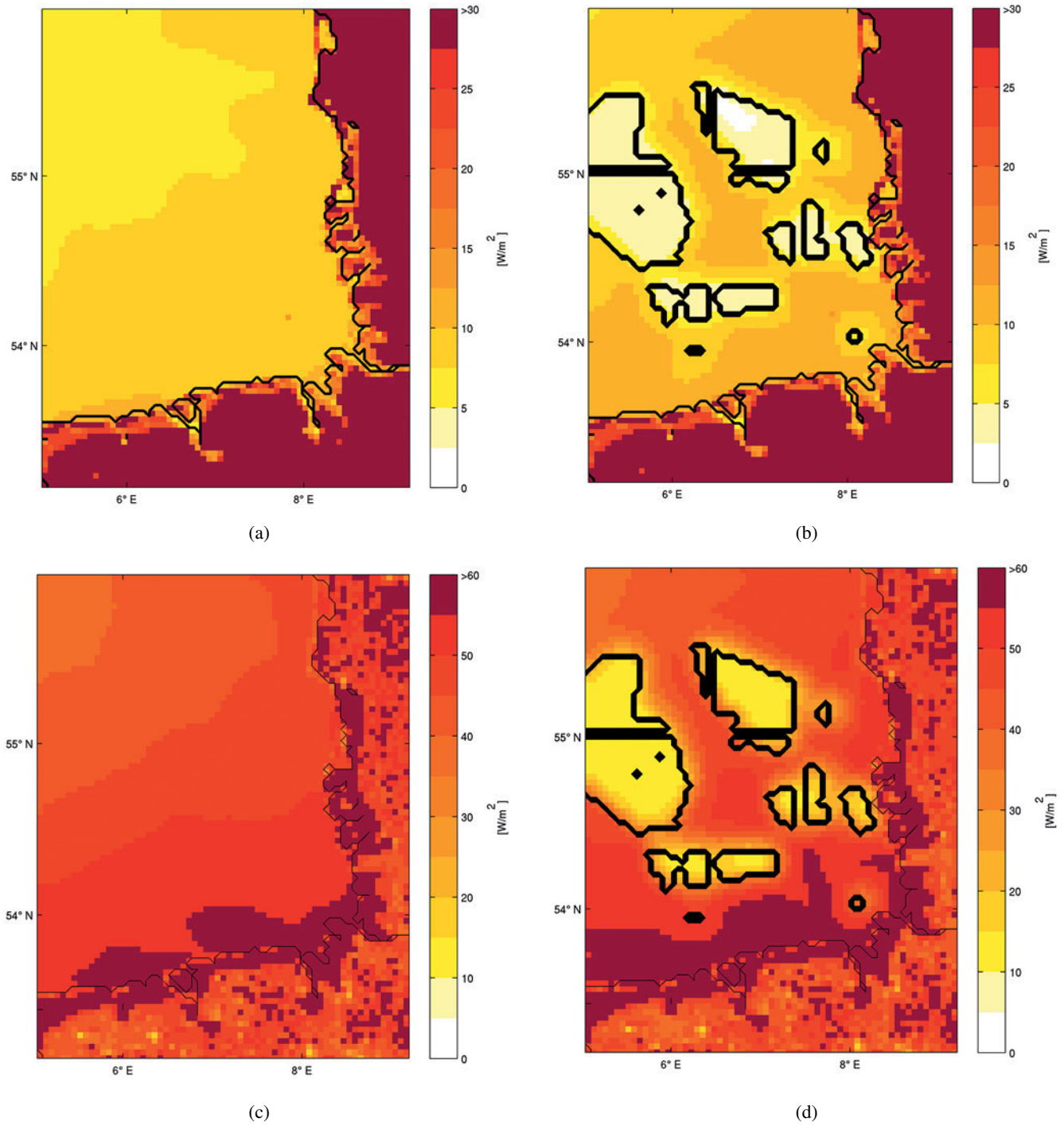

Figure 4: Mean sensible heat flux (a), (b) and mean latent heat flux (c), (d) between sea surface and atmosphere for averaged summer climate in the German Bight from (a), (c) reference simulations and (b), (d) scenario simulations. Positive values are defining fluxes from the ocean to the atmosphere.

The air temperature is highly impacted by the cloud developing and therefore the total air mass water content. Thus, to simulate the mean latent heat flux for the German Bight is important. The mean latent heat flux shows the same pattern as the sensible heat flux but in the range of 35 W/m^2 to 60 W/m^2. Figure 4c shows the simulated mean latent heat flux for the reference simulations. The result fits with the data from Michaelsen et al. (1998). Therefore, the chosen 40 days are representative for the mean sensible and latent heat flux in the German Bight during summer months as well as for wind speed and temperature frequency distribution.

3 Results

To determine the influence of the wind farms, each weather situation is simulated twice, with and without

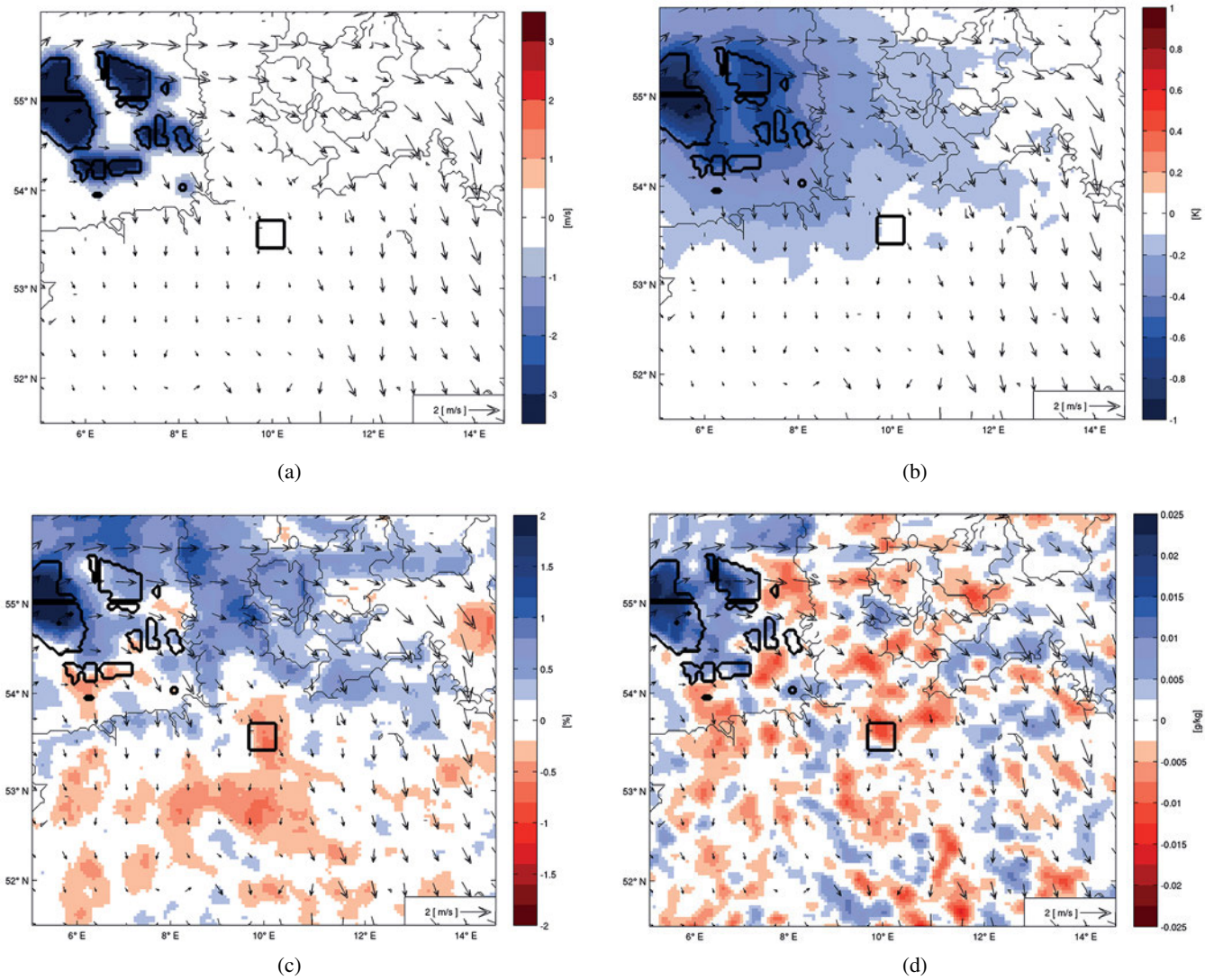

Figure 5: Mean differences in (a) wind speed, (b) temperature and (c) relative humidity at 10 m above surface and (d) integral cloud water content between scenario and reference simulations for averaged summer climate. Hamburg is located in the domain centre and marked with a black frame. The wind farms in the German Bight are also outlined with black frames and located in the North-West quadrant of the model domain. The vectors illustrate the mean wind velocity for the reference simulations, every 11th vector is shown.

wind farms in the German Bight. The latter is here denominated as "reference case", while the case that considers wind farms is named "scenario". The model simulations are evaluated with focus on simulation results in 10 m above ground to estimate the impact of the offshore wind farms on close to surface meteorology. The main target variable is the temperature in 10 m above ground. Other variables are studied to determine the reasons for changes in the temperature. The model results are stored every 30 minutes and results from midnight to midnight of the last 48 hours of each model simulation are used. Only those results are considered that are at least ten grid cells from the lateral boundaries. This shall avoid direct effects from nudging. The impact of the wind farms on different weather situations in the German Bight area is analysed in Section 3.1. The impact on the regional climate is investigated in Section 3.2. The impact on the climate of Hamburg is analysed in Section 3.3.

3.1 Impact of the wind farms on the meteorology for the different weather situations

Differences in temperature between the scenario and the corresponding reference case appear in all simulated weather situations and also in the summer climate average (Figure 5b). The changes in the temperature are, however, not restricted to the area of the wind farms but in average and in most weather situations simulated in a much larger area. In most cases, the flow upwind and lateral to the wind farms is also affected, not only the flow downwind. In some cases, the wind speed in the wind farm areas is temporarily lower than the cut-in wind speed of 2.5 m/s and the wind farms switch off. Then the differences in the temperature between scenario and the corresponding reference case decrease. Some hours after cut-off, the impact inside the model domain has nearly

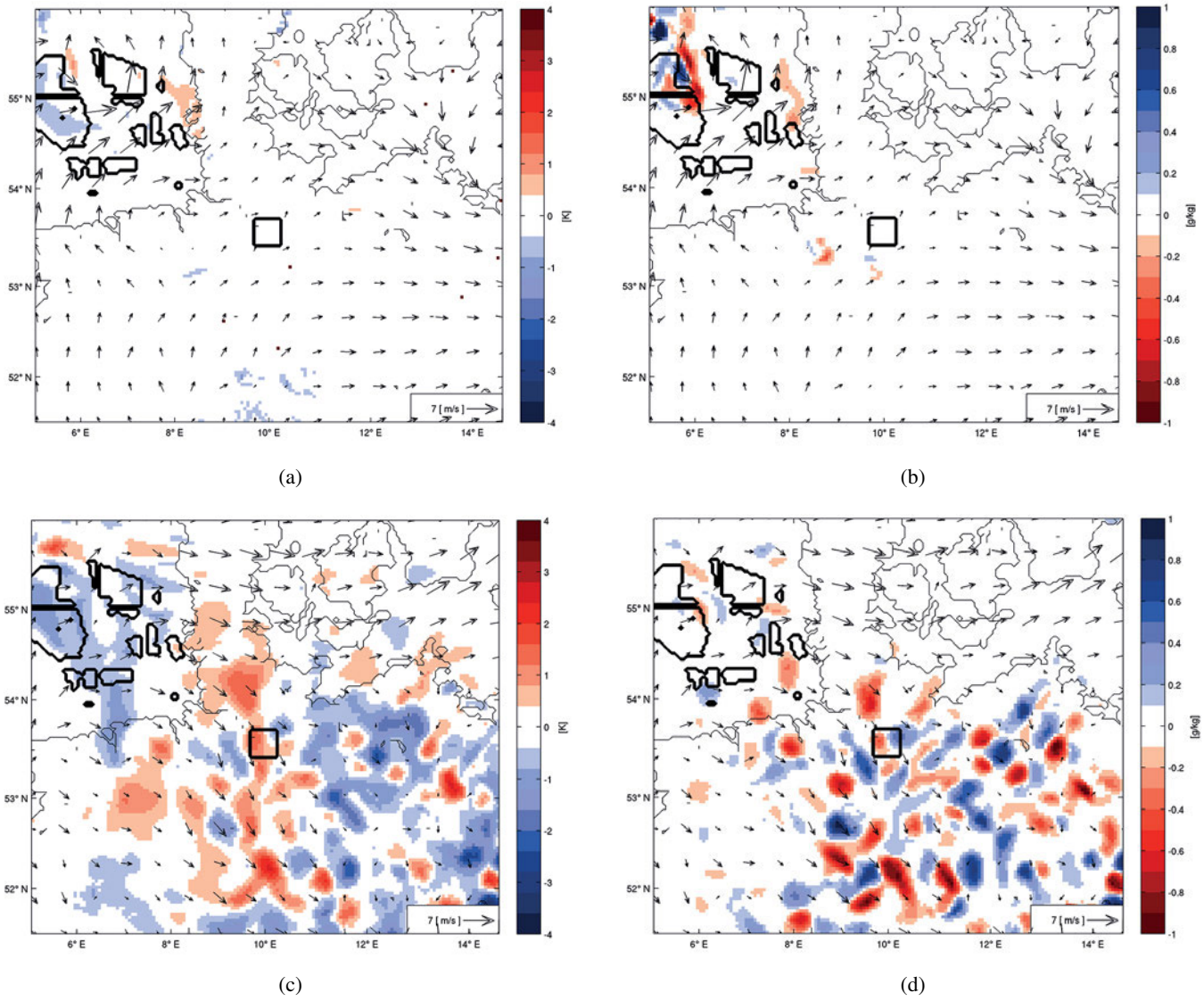

Figure 6: Differences in (a), (c) temperature at 10 m above surface and (b), (d) integral cloud water content between scenario and reference simulations for (a), (b) WP6C at 0000 LT and (c), (d) WP1C at 1800 LT of the last day of simulation. Hamburg is located in the domain centre and marked with a black frame. The wind farms in the German Bight are also outlined with black frames and located in the North-West quadrant of the model domain. The vectors illustrate the instantaneous wind velocity for the reference situations, every 11th vector is shown.

disappeared (Figure 6a, 6b). In the simulations used in this study, the wind speed is lower than the cut-in velocity for only few hours. Additional simulations not used in this study, have lower wind speed and show no effect of wind turbines, neither at instant time nor in few hours mean (not shown).

If the wind speed is higher than the cut-in velocity, the impact of the wind farms is found in a large area. The effects depend on the weather situation. The impact differs from local effects to large scale temperature changes or from large scale cloud development to local cloud dispersal. In most but not in all cases, the effects are scattered and only local and not uniformly distributed.

As a result of the changed temperature and relative humidity, the cloud cover over the German Bight changes as well. Depending on the weather situation, sometimes sea fog is generated or existing sea fog is extended in the horizontal and vertical dimension. In other weather situations, convective clouds are shifted in space and time. In some weather situations, new clouds are generated and change the temperature field in such a way that clouds in other areas disappear. As an example, the pattern of convective cloud development is changed in WP1C, therefore local warming and cooling alternates (Figure 6c, 6d). Thus, not only cooling but in some weather situations also local warming is possible as a result of wind farms in the German Bight. Some further examples of the effects of wind turbines in different WPs are shown in Eichhorn (2013).

3.2 Impact of wind farms on regional climate

For analysing the impact of large wind farms on regional climate, the differences between each scenario

and its corresponding reference case are averaged over all weather situations. As shown in Section 2.4, the regional summer climate is sufficiently represented by the averaging approach.

The largest differences in wind speed between the scenario and reference cases were found within and close to the wind farms (Figure 5a). Here the largest decrease in wind speed is simulated reaching up to 3 m/s in the summer climate average. An underflow with high wind speed close to the ground in the near wake is not obtained in this study, because the grid resolution of $4\times4\,km^2$ do not represent the near wake. In the far wake, the underflow is eliminated by the vertical exchange. The decreases in wind speed in the areas around the wind farms are small and within ±0.5 m/s.

As shown in Figure 4a, the mean sensible heat flux is slightly positive, meaning the atmosphere gets warmed by the sea surface in the German Bight. The reduced wind speed in the wind farm area results in a decrease of the mean sensible heat flux in the same area (Figure 4b). This leads to lower air temperatures in 10 m above sea level in all scenario cases in the wind farm region and therefore in the summer mean in that area (Figure 5b). Based on the air temperature reduction, the temperature gradient between sea surface and air increases and counteract the reduction of the sensible heat flux. This effect is weaker than the effect of the reduced wind speed but becomes important in the area around the wind farms. Due to the in average lower temperature, the mean sensible heat flux around the wind farms becomes slightly higher but this can not counteract completely the decrease in temperature. The major effect in temperature is found inside the wind farm area but a large area over Northern Germany and Southern Denmark is affected (Figure 5b). As mentioned in Section 3.1, dependent on the weather situation, local warming and cooling occur due to changes in the cloud development. Even if the local warming in some weather situations may have the same magnitude as the cooling, on average the warming effect is small compared to the cooling (Figure 5b). In the climatological summer mean, the warming (below 0.1 K) is one order of magnitude smaller than the cooling (up to 1.0 K) and very local.

The changes in the latent heat flux between scenario (Figure 4d) and reference (Figure 4c) simulations are similar to the changes in the sensible heat flux (Figure 4). In climate summer average, the relative humidity is increased in the area of decreased temperature and decreased due to decreases in the total air mass water content in the remaining areas (Figure 5c). The differences in temperature and relative humidity are strongest within and close to the wind farm area. But unlike the changes in the wind speed, these effects are scattered over a larger area. The changes in temperature and total air mass water content cause also changes in the cloud development and therefore generate changes in temperature again. The differences of the mean integral cloud water content show cloud development in the wind farm area but scattered effects of cloud development and dispersal in the areas far away (Figure 5d). Thus, the changes in temperature, relative humidity and cloud development are more long-range than the changes in the wind speed. Because of the mean wind direction and the position of the wind farms, often large parts of the downwind area are located over land.

Table 1: Space and time averaged temperature differences between scenario and reference cases for the regions "wind farm", "upwind", "downwind", "lateral", "total" and "Hamburg" as mean values and separated for night (1800 LT–0530 LT) and day (0600 LT–1730 LT) as summer average.

region	mean [K]	night [K]	day [K]
wind farm	−0.55	−0.61	−0.48
upwind	−0.01	−0.02	−0.01
downwind	−0.17	−0.16	−0.18
lateral	−0.16	−0.17	−0.15
total	−0.23	−0.23	−0.23
Hamburg	−0.05	−0.01	−0.08

To determine the upwind and downwind as well as the lateral effects the wind farms have on the regional summer climate, the model domain around the wind farms is split into four regions. The first region is the wind farm area itself, which is the same for every weather situation. The wind farm area is extended about $200\times200,\,km^2$. The other three regions are determined for each half-hourly output time separately with respect to the instantaneous wind direction in the wind farm area. Their size is chosen to be the same as that of the wind farm region. This leads to areas up to 200 km upwind and 200 km downwind of the wind farm area for the upwind and downwind regions, respectively. The region lateral of the wind farm area is determined to extend 100 km towards each side of the wind farms. Some of the model domain boundaries are very close to the wind farm areas. Therefore, not every region is evaluated for each output time and sometimes the regions are evaluated in a smaller domain. This is considered in the space and time averaging. Analyses are separately done for nighttime and daytime. The nighttime is chosen from 1800 LT to 0530 LT and the daytime accordingly from 0600 LT to 1730 LT.

The space averaged time series are calculated for every region. For wind speed no diurnal cycle is found (not shown). The decrease in temperature between scenario and reference climate shows changes in the areas around the wind farms and the changes are time dependent. On average, a cooling with the magnitude of −0.23 K is found, values for day and night time do not differ (Table 1). Splitting the changes in temperature with respect to the different regions, the major mean cooling effect is found within the wind farm region (−0.55 K). The regions lateral and downwind are cooled with the magnitude of −0.16 K and −0.17 K respectively. The effect upwind of the wind farm area is small (−0.01 K). Separating the changes in night- and daytime averages for the different regions highlights different behaviours dur-

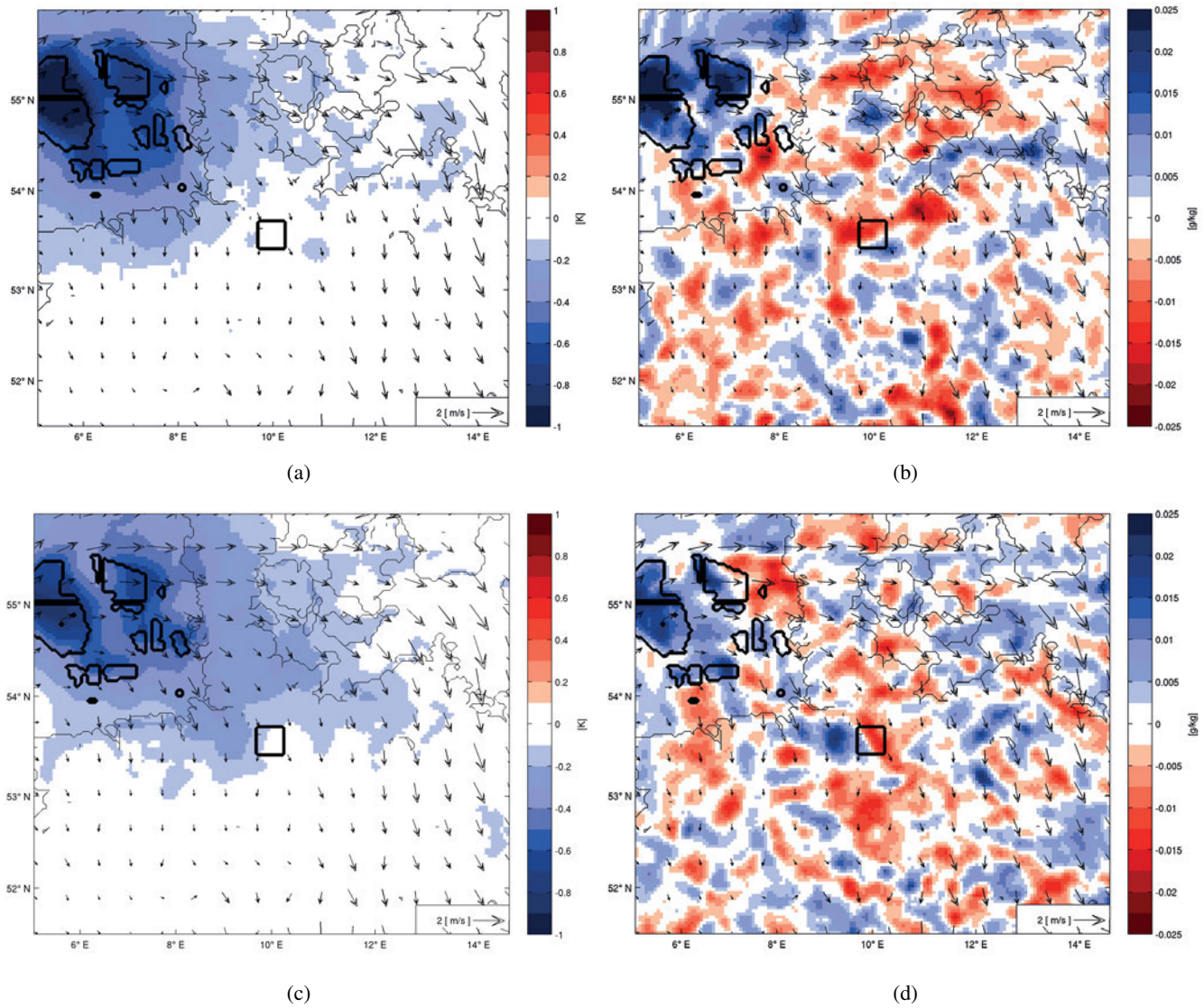

Figure 7: Same as Figure 5b and 5d but for (a), (b) nighttime and (c), (d) daytime temperature and integral cloud water content.

ing time of day. The largest differences are found again in the wind farm region, with cooling of −0.61 K during the night and −0.48 K during the day. The region lateral show slightly larger temperature decreases (−0.17 K) during night than during the day (−0.15 K). In the region downwind, the decrease of temperature is smaller during the night (−0.16 K) than during the day (−0.18 K). These diurnal effects are also apparent at night (Figure 7a) and day (Figure 7c) in the whole domain. The night-time patterns show a high magnitude inside and close to the wind farm area while the effect is only scattered for the distance. Even though the maximum magnitude of temperature reduction is smaller during day, the area of strong influence is larger. It is more than 0.3 K over Schleswig-Holstein which is very often in the downwind area due to the frequency of the weather situations with westerly winds. Consequently, the pattern of the daily mean (Figure 5b) is a superposition of both patterns. Even if the mean changes in the temperature are small, the simulations show that wind farms have an impact on regional climate. Hence the statistics for the summer climate are satisfied, the mean influence is real. In single situations, the impact can be much larger or nearly vanish.

The changes in the integral cloud water content show no diurnal cycle. The night- (Figure 7b) and daytime (Figure 7d) averages of the integral cloud water content are similar to the daily mean (Figure 5d).

3.3 Impact of the wind farms in the German Bight on the summer climate of Hamburg

Hamburg is situated roughly 100 km inland from the German Bight. As shown in Sections 3.1 and 3.2, the impact of the wind farms is quite long-range. Hamburg is located in the margins of the influenced region.

Analyses of the model results shows that the wind farms in the German Bight lead to in average slightly higher wind speed in the western part of Hamburg and to lower wind speeds in the southern and north-eastern part (Figure 8a). On average, the changes in wind speed

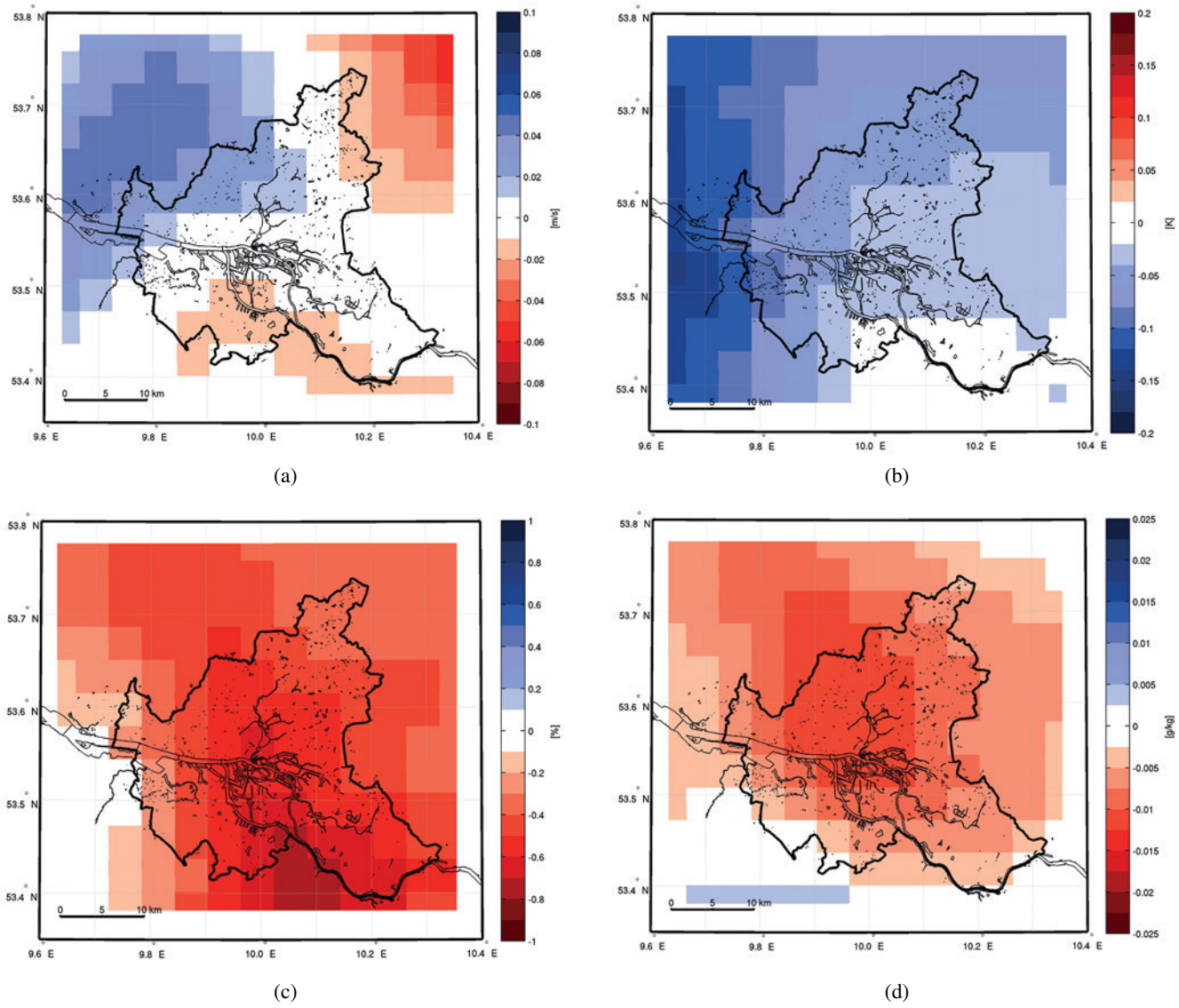

Figure 8: Mean differences in (a) wind speed, (b) temperature and (c) relative humidity at 10 m above surface and (d) integral cloud water content between scenario and reference simulations for summer climate average. Hamburg is marked with a thick black line and the thinner lines illustrate the water bodies of Hamburg.

are very small ($< \pm 0.1$ m/s) but in single situations, the pattern and the magnitude of the differences can be more pronounced. The regional wind climate as represented by the simulations is only marginally changed in Hamburg by the wind farms in the German Bight.

The changes in temperature are independent of the changes in wind speed (Figure 8b). A small cooling of up to -0.1 K is found that decreases from north-west to south-east. The wind farms in the German Bight also influence the relative humidity. In the area of Hamburg, it results in a small drying (≤ -1 %), mainly during the night (Figure 8c). In summer mean, Hamburg is located in an area of cloud dispersal. The decrease in the integral cloud water content (Figure 8d) counts up to 0.015 g/kg, about 10 % compared to the reference mean.

The changes impact the urban climate. Hoffmann et al. (2012) found a dependency of the UHI on wind speed, relative humidity and cloud cover. These variables are affected by the wind farms. Even if these changes are, except the cloud dispersal, in average and each for itself small, the interaction leads to changes of the UHI. The cloud dispersal increases the incoming solar radiation and therefore intensifies the UHI. The mean strong UHI is built for the evening hours from 2000 LT to 2400 LT as a difference between the city of Hamburg and model results averaged from two measurement sites in the rural surrounding (Hoffmann, 2012).

As discussed by Hoffmann (2012), the UHI pattern of the current conditions reflects the build-up density and the ground sealing of Hamburg but is also influenced by the river Elbe, which results in a slight warming (Figure 9a). The harbour areas and the high building density close to the river Elbe create the largest values for the UHI with a magnitude of up to 0.8 K. Note that these values are much smaller than the summer average value of 2.5 K based on Figure 10 of Schlünzen et al. (2010)

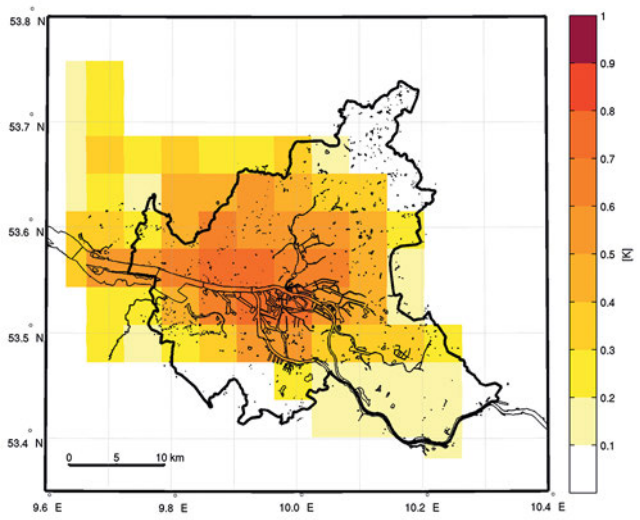

(a)

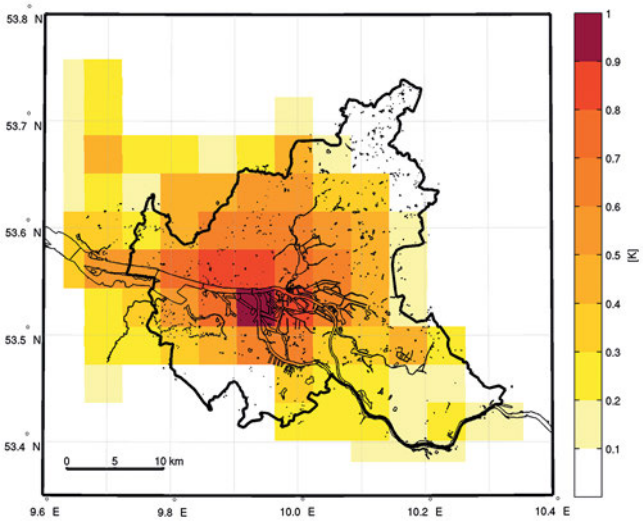

(b)

Figure 9: Mean strong UHI of Hamburg at 10 m above surface between 2000 LT and 2400 LT based on (a) the reference simulations and (b) the scenario simulations. Hamburg is marked with a thick black line and the thinner lines illustrate the water bodies of Hamburg.

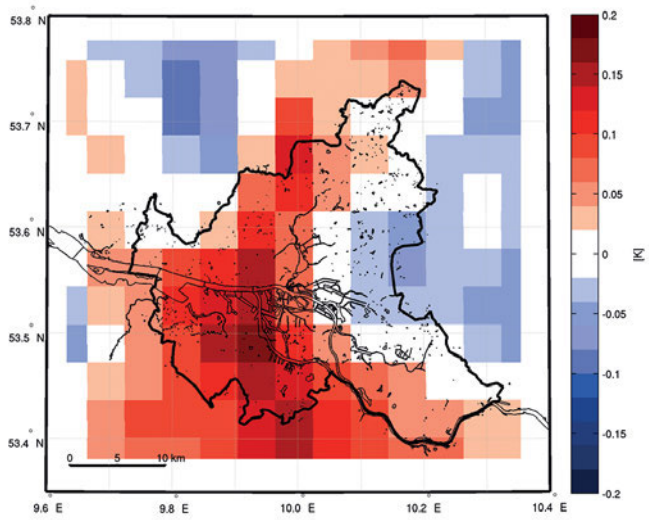

(a)

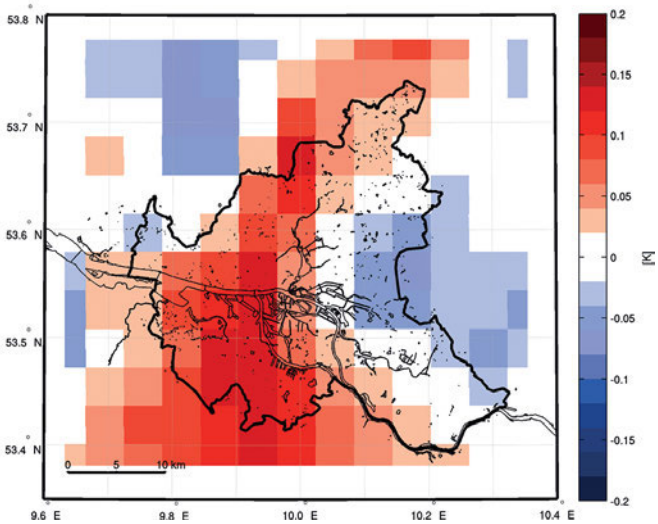

(b)

Figure 10: Differences of the UHI of Hamburg between (a) all the scenario and all the reference simulations and (b) only the most relevant weather situations WP1T, WP4T and WP6T at 10 m above surface between 2000 LT and 2400 LT. Hamburg is marked with a thick black line and the thinner lines illustrate the water bodies of Hamburg.

for the site of St. Pauli from measured data. This site is within the dense build-up part of the city and close to the river. However, it is not very representative and not comparable with a $4 \times 4\,\mathrm{km}^2$ summer average value as derived from the model results. The sub-urban areas in the southern and north-eastern parts of Hamburg show small UHI values with a magnitude of approximately 0.1 K.

To estimate the impact of the wind farms on the UHI, the UHI is calculated from the results of the scenario cases. The resulting UHI is shown in Figure 9b. The UHI, especially in the inner city, but also in the western and south-eastern parts of Hamburg is up to 0.2 K higher than for the reference case. In the eastern part of Hamburg the UHI decreases up to −0.1 K (Figure 10a). Therefore, even if the temperature in daily or night- or daytime mean decreases, the temperature difference between large areas of the city and the rural surroundings increases in the evening hours.

The changes in the mean strong UHI mainly result from the simulations conducted for the three weather situations WP1T, WP4T and WP6T. This is apparent if only these situations are used to calculate the differences as shown in Figure 10b, which is only based on changes resulting from these three cases. Changes of the UHI up to ±0.2 K in these three WP occur (Figure 11) while the changes in the other WP are small (≤ ±0.02 K).

Summarising, the average of these three patterns reflects the average changes well. The urban effect becomes more important in the scenarios with large offshore wind farms. In average, the UHI increases because of the cloud dispersal even if the changes in the other meteorological variables are in average small. The ur-

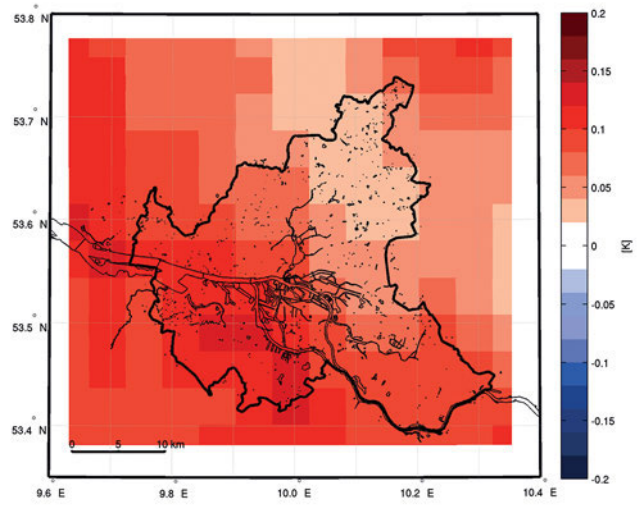

(a)

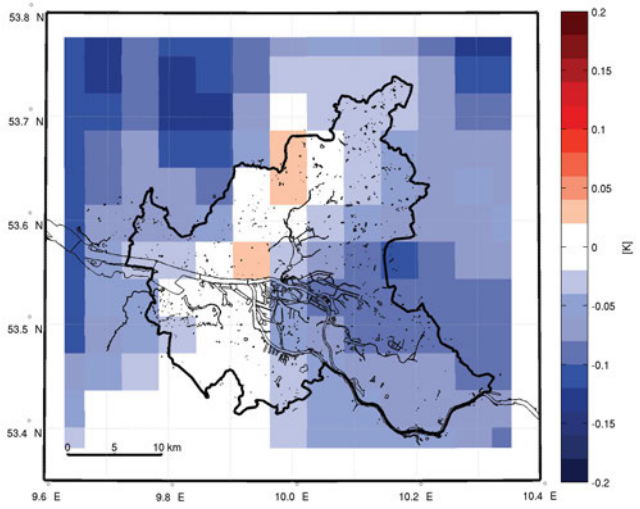

(b)

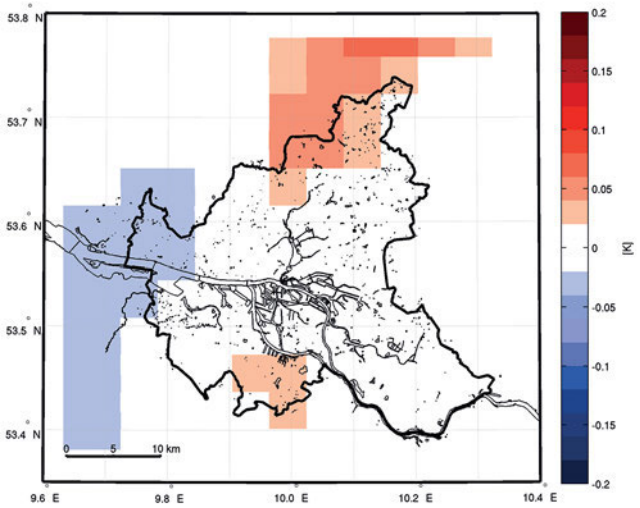

(c)

Figure 11: Differences of the UHI of Hamburg between the scenario and the reference simulations of the most relevant weather situations (a) WP1T, (b) WP4T and (c) WP6T at 10 m above surface between 2000 LT and 2400 LT. Hamburg is marked with a thick black line and the thinner lines illustrate the water bodies of Hamburg.

ban effects should be reduced, so that the cooling of the wind farms remains noticeable as a slight cooling for Hamburg (Figure 8b). All in all, the impact of 100 km away offshore wind farms on the urban climate is not negligible.

4 Conclusions

In the present study, the influences of large wind farms in the German Bight on regional and urban climate are investigated using the non-hydrostatic, three-dimensional, numerical model METRAS, which is now extended for the representation of wind turbines with the actuator disc concept. In the present study, simulations are performed for the current situation and for a scenario with large wind farms in the German Bight. The impact is analysed not only in the wind farm area itself or in its direct wake but also for 100 km apart from the wind farms. Hereby, this study closes the gap between several local (Baidya Roy et al., 2004; Baidya Roy and Traiteur, 2010; Baidya Roy, 2011; Christiansen and Hasager, 2005; Zhou et al., 2012) and global studies (Keith et al., 2004; Miller et al., 2011; Wang and Prinn, 2010).

Due to the coarse grid resolution of 4 km used in the present study, several wind turbines are represented in one grid cell by a fraction of rotor area per grid volume. However, the high vertical resolution allows the consideration of the wind turbines in their corresponding height. Therefore, the momentum absorption is simulated in higher model levels and this only interacts with the flow field at the surface.

To represent the summer climate, 40 days from 20 characteristic weather situations are simulated and their results averaged. The selected weather situations represent the summer climate well. This was shown by comparing statistics of 30 years of data from 27 weather stations and determining the skill scores following Perkins et al. (2007).

The wind farms in the German Bight affect a large area inland. Because of changed surface fluxes within the wind farm area, temperature, relative humidity and cloud development change locally and on the regional scale. On average, the wind farms in the German Bight result in a cooling for Schleswig-Holstein, Hamburg, the north-eastern part of Lower-Saxony and the southern part of Denmark. These areas are located in the main wind direction and frequently downwind of the wind farms. The local warming found for some weather situations does not appear in the summer average, because this warming is very local and one order of magnitude smaller than the cooling. The intensity of the cooling, however, changes between night- and daytime. The largest impact is always found within the wind farms itself. Inside the wind farm areas and in the lateral area, the impact of the wind farms is larger during the night then during the day. This is reversed in the area downwind of the wind farms.

Hamburg is located about 100 km from the coast but still inside the area affected by the offshore wind farms. The wind speed and temperature are slightly decreased. Hamburg is located in the area of decreased relative humidity, generated by a decreased total air mass water content. The integral cloud water content decreases about 10 km compared to the reference mean. As shown by Hoffmann et al. (2012), the relevant variables for estimating the UHI of Hamburg are wind speed, cloud cover and relative humidity. All these variables are affected by the wind farms in the German Bight, and the UHI of Hamburg increases during evening hours even if the absolute value of temperature decreases in daily, night- or daytime mean. Therefore, the urban effects of Hamburg become more important when large offshore wind farms are installed in the German Bight. The temperature reduction found in this study supports the global results of Wang and Prinn (2010), who found global cooling caused by large scale wind farms if they are installed over water. The current results show that the same effect is true for the regional and, furthermore, that it might impact the development of summer urban heat islands.

Acknowledgments

This work is supported by the project KLIMZUG-NORD, funded under grant 01LR0805D by the German Federal Ministry of Education and Research and through the Cluster of Excellence 'CliSAP' (EXC177), University of Hamburg, funded through the German Science Foundation (DFG). Surface cover data and information on building characteristics have been retrieved from the "Freie und Hansestadt Hamburg, Landesbetrieb Geoinformation und Vermessung (Nr.102156)", the "Landesamt für Geoinformation und Landentwicklung Niedersachsen (LGN)", the "Landesvermessungsamt Schleswig-Holstein", the "Amt für Geoinformation" and the "Vermessungs- und Katasterwesen Mecklenburg-Vorpommern". Fees for these datasets were covered by the University of Hamburg as well as by the excellence cluster CLISAP. Meteorological data for model forcing have been provided by the ECMWF. Meteorological observation data were provided by the German Meteorological Service (DWD). The water surface temperatures are received from NOAA. Wind turbine and wind farm data have been provided by the "Zukunft Küste – Coastal Futures" project founded through the German Federal Ministry of Education and Research under grant 03F0476 A-C.

Appendix

Linde (2011) determined the thrust coefficient for a Nordex N80/2500 wind turbine from field measurements presented in Machielse et al. (2007). The thrust coefficients used in this study are decreased compared to the thrust coefficients from Linde (2011), because larger wind turbines seem to have lower power and thrust coefficients (Enercon, 2010).

Table 2: Thrust coefficient used in this study to parametrise the wind turbines.

wind speed [m/s]	thrust coefficient c_T
0.0	0.00
2.5	0.45
9.0	0.37
13.0	0.28
17.0	0.00

The model METRAS was tested with different thrust coefficients. The result showed that METRAS results with the coarse grid resolution of $4 \times 4\,\mathrm{km}^2$ used in this study, are nearly independent from the thrust coefficient. Therefore, the thrust coefficients given in Table 2 are considered to be sufficiently determined.

References

Baidya Roy, S., 2011: Simulating impacts of wind farms on local hydrometeorology. – J. Wind Engin. Indust. Aerodyn. **99**, 491–498.

Baidya Roy, S., J.J. Traiteur, 2010: Impacts of wind farms on surface air temperatures. – Proceedings of the National Academy of Sciences **107**, 17899–17904.

Baidya Roy, S., S.W. Pacala, R.L. Walko, 2004: Can large wind farms affect local meteorology?. – J. Geophys. Res. **109**, 1–6.

Becker, G.A., 1981: Beiträge zur Hydrographie und Wärmebilanz der Nordsee. – Deutsche Hydrografische Zeitschrift **34**, 167–262.

Burkhard, B., 2006: Nordsee 2055 – Zukunftsszenarien für die Küste. – EcoSys Suppl. Bd. **46**, 70–89.

Christiansen, M.B., C.B. Hasager, 2005: Wake effects of large offshore wind farms identified from satellite SAR. – Remote Sens. Environ. **98**, 251–268,.

Daschkeit, A., 2011: Das Klima der Region und mögliche Entwicklungen in der Zukunft bis 2100, in von Storch, H. and Claussen, M. and KlimaCampus Team. – Klimabericht für die Metropolregion Hamburg. Berlin, Heidelberg: Springer Verlag, 61–90.

ECMWF, 2009: Part II: Data assimilation. – IFS DOCUMENTATION – Cy33r1 Operational implementation 3 June 2008, 160 pp.

ECMWF, 2010: Part VII: Data assimilation. – IFS DOCUMENTATION – Cy36r1 Operational implementation 26 January 2010, 168 pp.

Eichhorn, A., 2013: Determining reasons for impacts of offshore wind farms on meteorological parameters in North-Western Germany. – Bachelorarbeit Meteorologie, Univ. Hamburg.

El Kasmi, A., C. Masson, 2008: An extended $k - \varepsilon$ model for turbulent flow through horizontal-axis wind turbines. – J. Wind Engin. Indust. Aerodyn. **96**(1), 103–122.

Emeis, S., 2010: A simple analytical wind park model considering atmospheric stability. – Wind Energy **13**, 459–469.

Enercon, 2010: ENERCON Windenergieanlagen. – Produktübersicht.

Fitch, A.C., J.B. Olson, J.K. Lundquist, J. Dudhia, A.K. Gupta, J. Michalakes, I. Barstad, 2012: Local and mesoscale impacts of wind farms as parameterized in a mesoscale NWP model. – Mon. Wea. Rev. **140**, 3017–3038.

Fitch, A.C., J.K. Lundquist, J.B. Olson, 2013: Mesoscale influences of wind farms throughout a diurnal cycle. – Mon. Wea. Rev. **141**, 2173–2198.

Grawe, D., H.L. Thompson, J.A. Salmond, X.-M. Cai, K.H. Schlünzen, 2013: Modelling the impact of urbanisation on regional climate in the Greater London Area. – Int. J. Climatol. **33**, 2388–2401.

Gross, G., 2010: Numerical simulations to the diurnal variation of wakes behind wind turbines. – Meteorol. Z. **19**, 91–99.

Hau, E.W., 2002: Grundlagen, Technik, Einsatz, Wirtschaftlichkeit. – Springer, 792 pp.

Hoffmann, P., 2012: Quantifying the influence of climate change on the urban heat island of Hamburg using different downscaling methods. – Ph.D. thesis, University of Hamburg.

Hoffmann, P., K.H. Schlünzen, 2013: Weather Pattern Classification to represent the Urban Heat Island in present and future climate. – J. Appl. Meteor. Climatol.**52**, 2699–2714.

Hoffmann, P., O. Krueger, K.H. Schlünzen, 2012: A statistical model for the urban heat island and its application to a climate change scenario. – Int. J. Climatol. **32**, 1238–1248.

Huth, R., C. Beck, A. Philipp, M. Demuzere, Z. Ustrnul, M. Cahynová, J. Kyselỳ, O.E.O. E. Tveito, 2008: Classifications of atmospheric circulation patterns. – Ann. New York Academy Sci. **1146**, 105–152.

Keith, D.W., J.F. DeCarolis, D.C. Denkenberger, D.H. Lenschow, S.L. Malyshev, S. Pacala, P.J. Rasch, 2004: The influence of large-scale wind power on global climate. – Proceedings of the National Academy of Sciences of the United States of America **101**, 16115.

Lange, M., B. Burkhard, S. Garthe, K. Gee, A. Kannen, H. Lenhart, W. Windhorst, 2010: Analyzing coastal and marine changes: Offshore wind farming as a case study, Zukunft Küste – Coastal Futures Synthesis Report. – LOICZ Research and Studies No. **36**. GKSS Reasearch Center, Geesthacht **10**, 212 pp.

Linde, M., 2011: Modellierung des Einflusses von Windkraftanlagen auf das umgebende Windfeld. – Master's thesis, Meteorological Institute, KlimaCampus, University of Hamburg.

Lüpkes, C., K.H. Schlünzen, 1996: Modelling the arctic convective boundary-layer with different turbulence parameterizations. – Bound.-Layer Meteor. **79**, 107–130.

Machielse, L.A.H., P.J. Eecen, H. Korterink, S.P. van der Pijl, J.G. Schepers, 2007: ECN test farm measurements for validation of wake models. – Energy Research Centre of the Netherlands 12 pp.

Meyer, E.M.I., K.H. Schlünzen, 2011: The influence of emission changes on ozone concentrations and nitrogen deposition into the southern North Sea. – Meteorol. Z. **20**, 75–84.

Michaelsen, K., U. Krell, V. Reinhardt, H. Grassl, L. Kaufeld, 1998: Climate of the North Sea. – Selbstverlag des Deutschen Wetterdienstes, Offenbach am Main, Einzelveröffentlichungen Nr. **118**.

Mikkelsen, R.F., 2003: Actuator disc methods applied to wind turbines. – PhD Thesis, Technical University of Denmark 121 pp.

Miller, L.M., F. Gans, A. Kleidon, 2011: Estimating maximum global land surface wind power extractability and associated climatic consequences. – Earth Sys. Dyn. **2**, 1–12.

Molly, J.-P., 1978: Windenergie in Theorie und Praxis – Grundlagen und Einsatz – Verlag C.F. Müller, Karlsruhe, VII, 138, 2 S. Orig.-Broschur.

Perkins, S.E., A.J. Pitman, N.J. Holbrook, J. McAneney, 2007: Evaluation of the AR4 climate models' simulated daily maximum temperature, minimum temperature, and precipitation over Australia using probability density functions. – J. Climate **20**, 4356–4376.

Philipp, A., P.M. Della-Marta, J. Jacobeit, D.R. Fereday, P.D. Jones, A. Moberg, H. Wanner, 2007: Long-term variability of daily North Atlantic-European pressure patterns since 1850 classified by simulated annealing clustering. – J. Climate **20**, 4065–4095.

Pielke, R.A., 1984: Mesoscale Meteorological Modeling. – Academic Press, 612 pp.

Prospathopoulos, J.M., 2010: Discussion after a presentation at first WAUDIT summer school in Pamplona. – Personal communication.

Reynolds, R., N.A. Rayner, T.M. Smith, D.C. Stokes, W. Wang, 2002: An improved in situ and satellite SST analysis for climate. – J. Climate **15**, 1609–1625.

Schlünzen, K.H., 1990: Numerical studies on the inland penetration of sea breeze fronts at a coastline with tidally flooded mudflats. – Beitr. Phys. Atmos. **63**, 243–256.

Schlünzen, K.H., 1997: On the validation of high-resolution atmospheric mesoscale models. – J. Wind Engin. Indust. Aerodyn. **67**, 479–492.

Schlünzen, K.H., J.J. Katzfey, 2003: Relevance of sub-grid-scale land-use effects for mesoscale models. – Tellus A **55**, 232–246.

Schlünzen, K.H., U. Krell, 2004: Atmospheric parameters for the North Sea: a review. – Senckenbergiana maritima **34**, 1–52.

Schlünzen, K.H., T. Stahlschmidt, A. Rebers, U. Niemeier, M. Kriews, W. Dannecker, 1997: Atmospheric input of lead into the German Bight – a high resolution measurement and model case study. – Marine Ecol. Prog. Ser. **156**, 299–309.

Schlünzen, K.H., P. Hoffmann, G. Rosenhagen, W. Riecke, 2010: Long-term changes and regional differences in temperature and precipitation in the metropolitan area of Hamburg. – Int. J. Climatol. **30**, 1121–1136.

Schlünzen, K.H., D. Grawe, S.I. Bohnenstengel, I. Schlüter, R. Koppmann, 2011: Joint modelling of obstacle induced and mesoscale changes – Current limits and challenges. – J. Wind Engin. Indust. Aerodyn. **99**, 217–225.

Schlünzen, K.H., D.D. Flagg, B.H. Fock, A. Gierisch, V. Reinhardt, C. Spensberger, 2012: Scientific documentation of the multiscale model system M-SYS (METRAS, MITRAS, MECTM, MICTM, MESIM). – MEMI Technical Report 4. Meteorologisches Institut, KlimaCampus, Universität Hamburg 138 pp.

Stütz, E., G. Steinfeld, D. Heinemann, J. Peinke, 2012: Parametrisierung von Windparks in COSMO. – Abstract METTOOLS VIII, Mitteilungen aus dem Institut für Meteorologie der Universität Leipzig **49**, 15.

von Salzen, K., K.H. Schlünzen, 1999: A prognostic physico-chemical model of secondary and marine inorganic multicomponent aerosols I. model description. – Atmos. Environ. **33**, 567–576.

von Salzen, K., M. Claussen, K.H. Schlünzen, 1996: Application of the concept of blending height to the calculation of surface fluxes in a mesoscale model. – Meteorol. Z. **5**, 60–66.

Wang, C., R. . Prinn, 2010: Potential climatic impacts and reliability of very large-scale wind farms. – Atmos. Chem. Phys. **10**, 2053–2061.

Zhou, L., Y. Tian, S. Baidya Roy, C. Thorncroft, L.F. Bosart, Y. Hu, 2012: Impacts of wind farms on land surface temperature. – Nature Climate Change **1505**, 1–5.